

Analysis and mitigation of the carrier phase delay effect of the digital phase generated carrier algorithm

LI SHUWANG,^{1,2} SHAO SHIYONG,^{1,*} MEI HAIPING,¹ HAO QILONG^{1,2} AND RAO RUIZHONG^{1,2}

¹Key Laboratory of Atmospheric Composition and Optical Radiation, Anhui Institute of Optics and Fine Mechanics, Chinese Academy of Sciences, Hefei, Anhui 230031, China

²Science Island Branch of Graduate School, University of Science and Technology of China, Hefei, 230026, China Publications

*Corresponding author: shaoshiyong@aiofm.ac.cn

Received XX Month XXXX; revised XX Month, XXXX; accepted XX MonthXXXX; posted XX Month XXXX (Doc. ID XXXXX); publishedXX Month XXXX

We present an improved digital phase generated carrier (PGC) algorithm based on the synchronous carrier restoration(SCR) method to mitigate the carrier phase delay effects. The most distinguishing feature of this method is that it picks up the carrier signal information (frequency and phase) from the interference signal directly and accomplishes the processing of carrier signal restoration synchronically. In comparison with the traditional one which adopts the initial carrier signal, the total-harmonic-distortions of the SCR method is only 0.091%, lower than the traditional one's 18.38%, and the signal-to-noise-ratio increases 29 dB. Further, we derive the analytic expression of distortion component and verify it by experiments. This technique may be potentially applied in a long distance large-scale distributed fiber-optic interferometer sensors array. © 2016 Optical Society of America

OCIS codes:(060.5060) Phase modulation; (060.2300) Fiber measurement; (120.3180) interferometry

<http://dx.doi.org/10.1364/AO.99.099999>

1. Introduction

Fiber-optic interferometer sensor (FOIS) such as Mach-Zehnder, Michelson and Sagnac interferometers is the most sensitive class in all kinds of fiber sensors. It can output a linearly signal and give much higher performance than conventional electronic sensors [1,2]. FOIS also has the features of compact size, light weight, wide responsive bandwidth and immunity to electromagnetic interference [3]. Additionally, it is very suitable for long distance large-scale distributed sensing due to the very small propagation loss of in fiber and ease of multiplexing [4]. Hence, FOIS is widely used in fields of weak signal detection (i.e sound pressure, magnetic, acceleration and vibration) [1]. Generally, PGC algorithm is the most widely used signal demodulator of FOIS [5], due to its advantages of high resolution, high sensitivity, wide dynamic range, good linearity and the multi-channels demodulated capability [6]. In PGC algorithm, a high-frequency sinusoidal phase modulation signal is applied to the FOI to generate a phase carrier, this will up-convert the sensing signal onto the sidebands of carrier frequency. Then, a pair of quadrature components containing the sensing signal are obtained by mixing the interference signal with the carrier signals [7]. Accordingly, if phase difference exists between the interference signal and the carrier mixing signals, the demodulated sensing signal will be distorted [4]. Moreover, this will be more serious for the long distance large-scale distributed sensing array because the

phase difference may be induced by the laser transmission time in leading and sensing fiber or the conversion time between analog and digital.

To mitigate above effects and improve the performance of FOIS, in this paper, we will analyze the distortion component of the demodulated signals induced by the carrier phase delay effect theoretically and experimentally. Then, an improved digital PGC algorithm based on the synchronous carrier restoration (SCR) method will be presented to mitigate this effect. The most distinguishing feature of this method is that it picks up the carrier signal information (frequency and phase) from the interference signal directly and accomplishes the processing of carrier signal restoration synchronically. Furthermore, an experimental system will be to verify the validity of the improved digital PGC algorithm. Results show that this method will eliminate the phase difference between the carrier signal and the interference signal and mitigate the phase delay effect.

The structure of this paper is as follows: In Section 2, we introduce the basic theory of PGC algorithm and analyze the effect of phase delay in PGC-Arctan algorithm. In Section 3, principle of the improved digital PGC algorithm based on the synchronous carrier restoration method is reported. In Section 4, we describe the experiments and results to evaluate the performance of this method and validate the previous

theoretically analysis. Finally, we summarize our conclusion in Section 5.

2. Analysis of the carrier phase delay effect

For the dual beam interferometer, after the carrier term is added, the output light intensity of interferometer can be shown as [7]

(1)

where A is the average interference intensity, B is the interference intensity, C is the PGC carrier phase modulation depth, ω_c is the angular frequency of carrier, s is the sensing signal, and ϕ_0 is the initial phase of interferometer.

In PGC algorithm, to recover the sensing signal from the interference signal in Eq. (1), a pair of quadrature components

After filtered by two low-pass filters to remove the terms above the highest frequency of interest, the quadrature components Eq. (6) and Eq. (7) are got

(6)

(7)

Obviously, two additional factors of α and β appears in and . In fact, they are the attenuation coefficient induced by phase delay. For the PGC-Arctan algorithm, after dividing Eq. (6) with Eq. (7) and arc tangent function processing, the result can be written as [8]

(8)

Here, the carrier phase modulation depth is just under 2.63 rad., accordingly, Eq. (8) can be modified to

(9)

The first term on the r. h. s. of Eq. (11) is DC component, which can easily be removed by a high-pass-filter. The second term is the desired sensing signal at the fundamental frequency. The third term and fourth term are even and odd harmonics, respectively.

Here, we adopt the total-harmonic-distortions (THD) to evaluate the carrier phase delay effect of PGC-Arctan algorithm which can

This indicates that the THD depends on the carrier phase delay, the sensing phase signal and the initial phase of interferometer. Further, we also adopt signal-to-noise-and-distortion (SINAD) to evaluate the carrier phase delay effect of PGC-Arctan algorithm. In this

The relationships of THD, SINAD and with different are plotted in Fig. 1., and of , , , and , and ranges from 0 to are chosen. If the initial phase of interferometer , we can see that when the phase delay approaches to (is odd number), THD increases rapidly, and when the phase delay is around (is even number), THD approaches to zero. Further, if the initial phase of interferometer , THD presents a different tendency. When the phase delay approaching to (is 2, 6), THD increases sharply, and when the phase delay is around (is 1, 3, 4, 5, 7), THD approaches to zero. It should be stated that when is (is 1, 2, 3, 5, 6, 7), the THD will get its maximum value of , and the SINAD will approach to . Specifically, the demodulation process will be failed. Here, in order to present more details of THD, these points are not shown. As a whole, THD is non-zero except for several special points, it

containing the sensing signal is obtained by mixing the interference signal with the carrier fundamental and second-harmonic signal, respectively. In actual, if considering the existence of conversion time delay from analog to digital and laser transmission time delay in fiber (leading fiber and sensing fiber), Eq. (1) should be modified as

(2)

here, τ is the time delay, $\delta\phi$ is the phase delay between the interference signal and initial carrier signal. Consequently, Eq. (3) can be obtained after using the Bessel function to expand Eq. (2) as follows

(3)

where n is the orders of Bessel function. Then, if multiply Eq. (3) with the initial carrier fundamental signal and second-harmonic signal, respectively, Eq. (4) and Eq. (5) can yield

(4)

(5)

In order to analyze effects of carrier phase delay of PGC-Arctan demodulation, we expand Eq. (9) into the fundamental component and the distortion component. Therefore, the can be written as

(10)

The first term on the right-hand side (r. h. s.) is the desired signal of the fundamental component. The second term is the initial phase of interferometer which can easily be removed by high-pass-filter. The third term is the distortion component, which is concerned with the carrier phase delay , the sensing phase signal and the initial phase of interferometer. If , the third term will disappear and the distortion will no longer exist. Moreover, if , the demodulated signal will be zero.

To investigate the harmonic distortion due to the phase delay, we assume that the sensing signal , and are the amplitude and the frequency of the sensing signal, respectively. Substituting the single-frequency sensing signal to Eq. (10) and using Bessel expansion, Eq. (10) can be written as [5]

(11)

represent the degree of harmonic distortion of demodulation signals. In this paper, THD is defined as the ratio of equivalent root-mean-square (RMS) amplitude of all harmonics to the amplitude of the fundamental component [5]. The analytic expression of the THD of the PGC-Arctan algorithm can be expressed as

(12)

paper, SINAD is defined as the ratio of the power of the fundamental frequency to the sum of the powers of all noise and harmonics [5]. Since is periodic, the fundamental component and the distortion component are periodic, too. Hence, the SINAD can be expressed as [8]

(13)

means that the distortion of demodulation signal is always existence. The relevant SINAD proofs the conclusion.

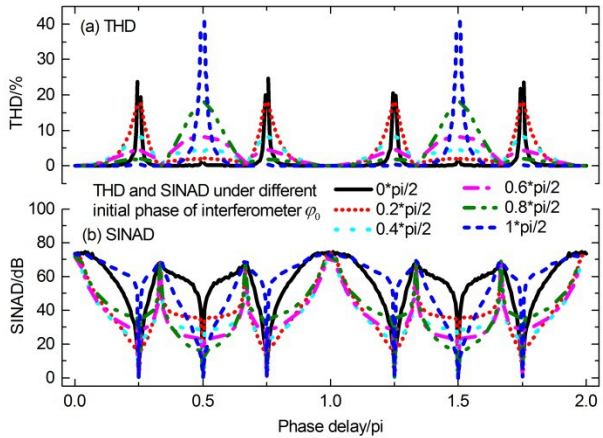


Fig. 1. The relationships of THD, SIAND and phase delay with different initial phase of interferometer.

Distortions of PGC-Arctandemodulated signals under and are shown in Fig. 2., andof,, , and . We can find that when the phase delay , the THD is %, the SINAD is , and the demodulated signal present a standard sinusoidal signal which is well coincided with the sensing signal. When the phase delay , the THD is %, but the SINAD is only which decreased , obviously, the amplitude of demodulated signal increased. When the phase delay , the THD sharply increases to %, the SINAD is only. It is clearly that the demodulated signals present a serious distortion both the amplitude and the waveform.

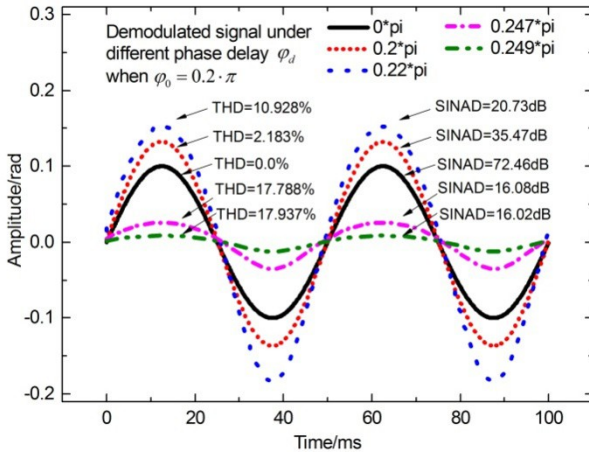


Fig. 2. Distortion of PGC-Arctan demodulation signals under different phase delay when the initial phase of interferometer.

3. Principle of the improved digital PGC algorithm based on the SCR method

Obviously, the existence of phase delay will cause serious effects of PGC algorithm. It is indispensable to eliminate the carrier phase delay. Here, we present a novel method based on synchronous carrier restoration which can eliminate the phase difference between the interference signal and the carrier mixing signal.

The frequency-domain interference signal is shown in Fig. 3, which is acquired from the experimental instrument shown in Fig. 6. The frequency of the carrier signal is and the sample rate is .

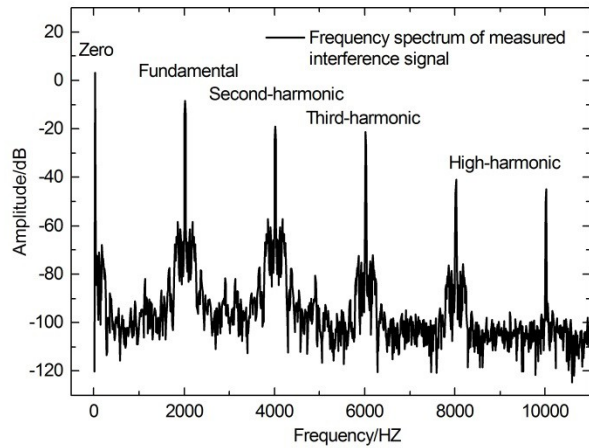


Fig. 3. Frequency-domain interference signal acquired from the experimental instrument.

From Fig. 3, we can see that the interference signal has the frequency components of zero, fundamental, second-harmonic and high-harmonic, et al. This is well coincided with the Bessel function of interference signal in Eq. (3). Consequently, if the Eq. (3) is filtered by two band-pass filters whose center frequency is fundamental and second-harmonic, respectively, the residual components can be written as

$$(14)$$

$$(15)$$

If ignore the effect of , Eq. (14) and Eq. (15) are the ideal source of carrier mixing signal. Because they are directly filtered from the interference signal, and the phase delay in the interference signal will transfer to the carrier mixing signal. This can ensure the carrier mixing signals synchronous with the interference signal. Unfortunately, the effect of is inevitable and in mostly times the frequency components of is lower than the carrier signal. Consequently, this will lead low-frequency disturbance to the carrier mixing signals and trigger a negative effect on the demodulation process.

Based on this, we present a novel method which picks up the information of frequency and phase from Eq. (14) and Eq. (15) directly, and then restore the carrier mixing signals synchronously. The whole process of the improved PGC algorithm based on the synchronous carrier restoration method is shown in Fig.4. Firstly, the interference signal is divided into two channels. One channel is directly transported to the PGC demodulator and another is transported to the synchronous carrier restoration module. The later will go across a band-pass filter, and then transfer to frequency domain from time domain by windowed Fast Fourier Transform (FFT). In the frequency spectrum, the carrier signal occupies the absolute advantage. Consequently, we can easily pick up the carrier information (frequency and phase) with the extraction module of single frequency signal and input the frequency and phase to the signal restoration module. Finally, the carrier mixing signals of fundamental signal and second-harmonic signal are restored. Obviously, if multiply Eq. (3) with the restored ones, the two additional factors of and in Eq. (6) and Eq. (7) are no longer existence.

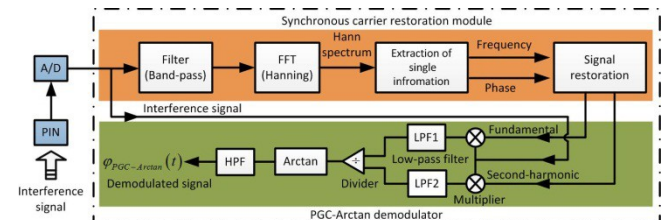


Fig.4. Schematic of improved digital PGC algorithm based on the synchronous carrier restoration method.

The feasibility of this algorithm is proved by the simulated demodulation without any noise. But there is no doubt that phase noise always exists in an actual interferometer and appears along with the sensing signal. So, it is indispensable to test the capability of the SCR method under different SNR and verify whether the phase noise will trigger an extra error on demodulated signal.

Here, we define the signal-to-noise-ratio (SNR) as

(16)

assuming that ϵ is uniform white noise, and SNR is from 0.1 to 10 by changing amplitude of ϵ . Further, we set $\omega_0 = 2\pi \times 10^6 \text{ rad/s}$, and the sample rate is 10^6 Hz . Simulative demodulation results based on the SCR method are shown in Fig. 5. From Fig. 5(a), we can see that when the SNR is greater than 5, the absolute error of φ_d equals zero which is picked up by the SCR method. When the SNR approaches to 0.1, the absolute error increased. Even so, the maximum absolute error is less than $1.75788 \times 10^{-3} \text{ rad}$ and the maximum standard deviation is only $1.75788 \times 10^{-3} \text{ rad}$. Further, we evaluate the influence of this small error, and result is shown in Fig. 5(b). The dot represents the THD of demodulated signals with theoretical predication, and the star represents THD of demodulated signals with the SCR method. We can find that the results under two circumstances are coincided well. The correlation coefficient is up to 0.999. This means that the SCR method can work well under low SNR, and only triggers a very small error. It is clear that this error has little effect on demodulated signal.

The SCR method directly picks up the carrier information (frequency and phase) from interference signal and accomplishes the carrier restoration processing synchronically. It means that the time delay of conversion time between analog and digital or the transmission time of laser in the leading fiber and sensing fiber has no effect on demodulation process. Because of the carrier mixing signal is originated from the interference signal. All the phase delay contains in the interference signal will transfer to the carrier mixing signal, too. Therefore, this method can ensure that the carrier mixing signal is completely matching with the interference signal.

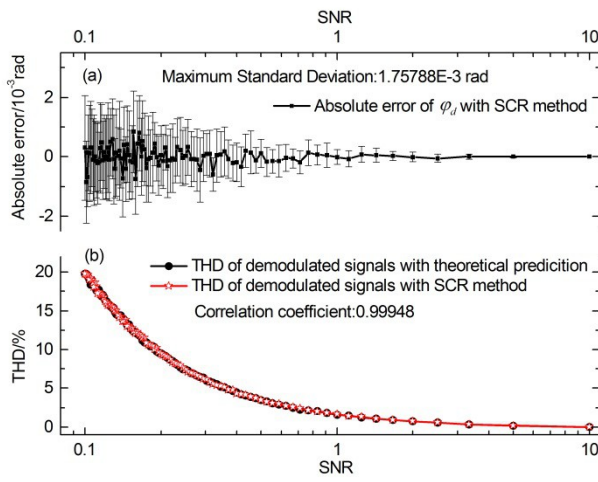


Fig. 5.Results of the synchronous carrier restoration method under different SNR.

4. Experiments and results

In order to verify the feasibility of synchronous carrier restoration method, the experiment instruments is set up as shown in Fig. 6 and Fig. 7. A modified Fizeau interferometer is employed in the experiment. A distributed-feedback semiconductor laser (NLK1B5EAAA, $\lambda = 1550 \text{ nm}$) is chosen as the light source. A sinusoidal phase carrier signal at the

frequency of 10^6 Hz is applied to the interferometer by directly current modulating the semiconductor laser to get the carrier phase signal. The carrier signal is generated by a signal generator (NI PXI-5406). The light is propagation in the single mode fiber. A fiber splitter is employed to separate the light passing through the fiber isolator into reference beam and several interference beams. The reference beam is directly detected by low-noise positive intrinsic-negative photodiode (PIN1), and this signal will be used to eliminate the laser intensity modulation (LIM) of interference signal [11,12]. A custom-made fiber collimator is employed to separate the interference beam passing through the fiber circulator into reference arm and signal arm. The light-emitting surface of collimator is plated a 30% reflecting film. So a part of light is reflected into the fiber again by the collimator reflecting film and back-propagation as the reference arm of interferometer. Others transmitted from the collimator and then penetrate into the collimator again after transferring the sensing area twice, due to the existence of reflector mirror which is handled by a piezoelectric transducer (PZT). This part is as the signal arm of interferometer. Consequently, the signal arm and reference arm are collinear actually and the arm path difference is nearly 20 cm. Therefore, interference pattern is created after they are combined, and then detected by photodiode (PIN2). The outputs of the photodiode are then sampled to simultaneously at the sampling rate of using a multifunction data acquisition card (NI PXIe-6366), and then transmitted into a computer to perform improved digital PGC demodulation algorithm with the synchronous carrier restoration method. The sample period is 10^{-6} s . This card has two digital-to-analog output channels, and the PZT control signal can output by it. The entire experiment instruments are placed on an optical bench supported by four air suspension legs.

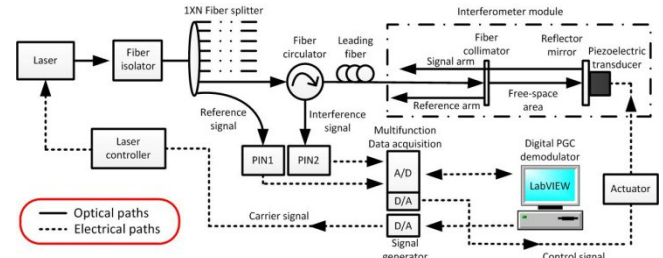


Fig. 6.Schematic of experimental instruments.

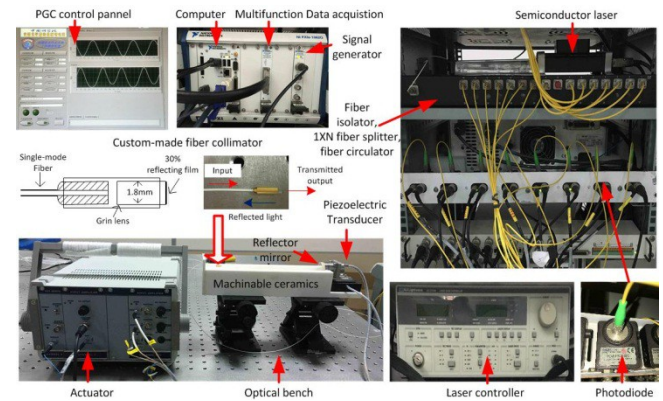


Fig. 7.Picture of experimental instruments.

4.1 Contrast of different carrier mixing signals

In experiment, we apply a stable sinusoidal voltage signal to the PZT which frequency is 10^6 Hz and amplitude is 10^{-3} m . This signal will be converted into a stable vibration signal and detected by the interferometer as shown in Fig. 6. The phase shift coefficient of the PZT is 10^{-3} rad/m . Further, two kinds of carrier mixing signals are got to demodulate the vibration

signal. They are the initial carrier signal from the PGC algorithm and the restoration carrier signal from the SCR method, respectively. From Fig. 9, we can see that the carrier mixing signal generated by the SCR method is completely matching with the interference signal. Different from this, the initial carrier signal has an obvious time delay with the interference signal. The time delay is major triggered by the conversion time of DAC and ADC. More concretely, the initial carrier signal is converted to analogue signal by a DAC and amplified before added into the FOI. Then, the interference light intensity of the FOI is converted to analogue signal by a photodiode, and further converted to digital signal by an ADC. After that, the interference signal will be combined with the initial carrier signal in digital PGC algorithm. It is obviously that, due to the existence of conversion time, the interference signal will have a time delay relative to the initial carrier signal, and this effect will be gradually accumulated. The carrier modulating period is , so the correspondence phase delay is , this will trigger a distortion component according to the former theoretical analysis in Eq. (10). Additionally, the laser transmission time can be ignored in our experiment, due to the length of the fiber (leading and sensing) is only about . This must be considered and will be more complex for a long distance large-scale distributed fiber-optic interferometer sensors array.

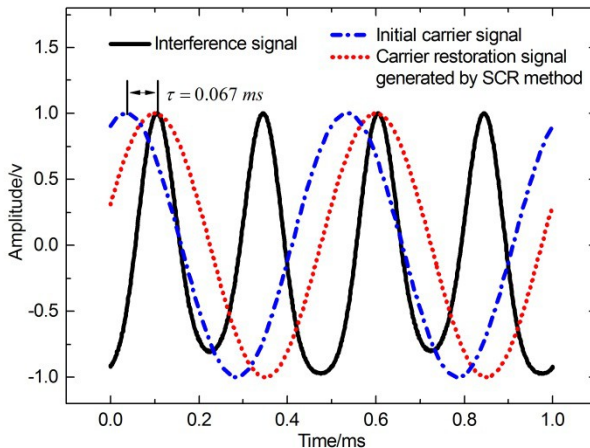


Fig. 9. Interference signal and carrier mixing signal which is produced by different methods.

Additionally, from Fig. 10, we can see that the corresponding demodulated signal with the initial carrier signal and the SCR method are different. The former present a good performance and is well coincided with the desired sinusoidal signal, the THD is only 0.091% and the SINAD is . In contrast, the demodulated signal with the initial carrier signal is seriously affected by the phase delay and presents an obvious distortion not only the amplitude but also the waveform. The THD is up to 18.3836% and the SINAD is only . More seriously, the symbol is opposite with the desired sinusoidal signal.

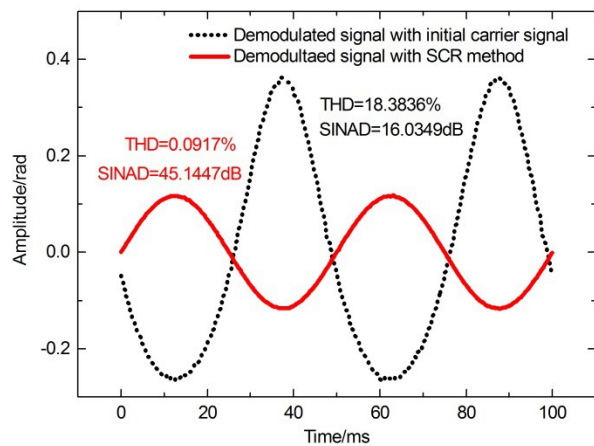


Fig.10. Demodulated results with different method.

4.2 linearity of the improved PGC algorithm based on SCR method

Furthermore, we linearly change the amplitude of sinusoidal voltage which is applied to the PZT to generate a linearly increase vibration signal. This vibration will be detected by the interferometer and demodulated by the improved PGC algorithm shown in Fig. 4. The details results are shown in Fig. 11, the demodulated signals present a good linearity performance, and the linear fitting correlation coefficient is up to 0.999. Results indicate that the system has a good linearity.

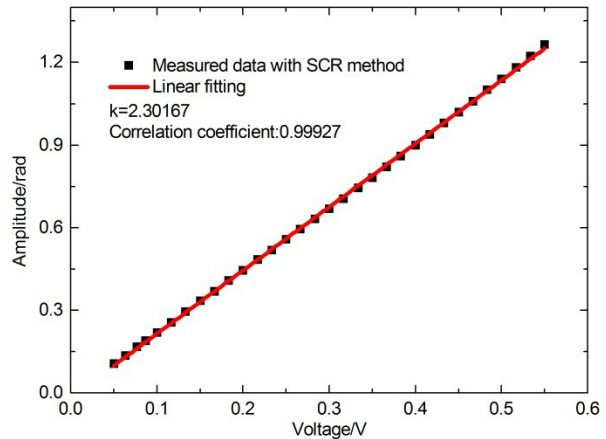


Fig.11.Voltage applied to PZT and demodulated phase signals.

4.3 Demodulated signals of PGC-Arctan under different phase delay

Moreover, in order to evaluate the performance of the SCR method and verify the theoretical analysis of distortion components, we assume the carrier mixing signal from the SCR method as the benchmark, and continue actively add phase delay step-by-step from 0 to into the interference signal, here, one step is . A stable single frequency sinusoidal signal at the frequency of is applied to the PZT, and other parameters are same just like above. With this method, we can get the experimental measured distortion component of PGC-Arctan algorithm induced by the carrier phase delay effects. At the same time, we also calculate the theoretical predicted ones by Eq. (14). The measured and theoretical predicted results are shown in Fig.12. We can see that the measured distortion component is in good agreement with the theoretical predicted ones, and the correlation coefficient is up to 0.99231 in the gray core area which includes the 90 percent of data.

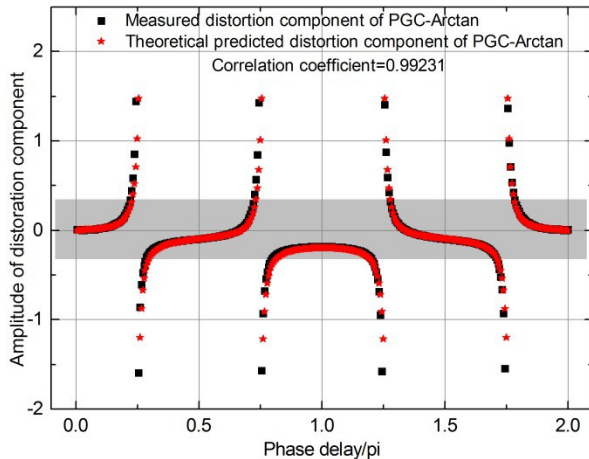


Fig. 12. Distortion component of measured and theoretical predicted one.

According to the results of the above experiments, the improved PGC algorithm based on the synchronous carrier restoration method can work well in an actual system, and the synchronous carrier restoration method can valid eliminate the phase delay effects and improve the performance of the FOIS system.

5. Conclusion

In this paper, an improved digital PGC algorithm based on the synchronous carrier restoration (SCR) method has been reported. Both the theoretical analysis and corresponding experiments have been carried out to investigate the carrier phase delay effect and the performance of SCR method. The carrier phase delay effect has been analyzed and the analytic expression of distortion component has been derived. The improved PGC algorithm based on the SCR method has demonstrated with the vibration measurement. Compared with the traditional PGC algorithm with initial carrier signal, it has a much lower THD as well as a better SINAD. A low THD of below 0.1% and a high SINAD of have been got for a small sinusoidal vibration signal induced by PZT. The demodulated signals with SCR method present a good linearity performance, and the linear fitting correlation coefficient is up to 0.999. With the improved digital PGC algorithm based on the synchronous carrier restoration (SCR) method, the performance of FOIS can be improved significantly.

Funding Information. National Science Foundation of China (NSFC) (41205022, 41475024, 41205010)

Acknowledgment. We thank Dr. Wenyue Zhu and Honghua Huang for their help and encouragements.

References

1. G. G. Thomas, A. B. Joseph, A. Dandridge, et.al. "Optical fiber sensor technology," *Transactions on Microwave and Techniques MTT-30(4)*, 472–499 (1982).
2. Y. Liu, L. W. Wang, C. D. Tian, et.al. "Analysis and optimization of the PGC method in all digital demodulation systems," *J. Lightw. Technol.* **26**(18), 3225–3233 (2008).
3. H. Xiao, F. Li, Y. L. Liu. "CrossTalk analysis of a fiber laser sensor array system based on digital phase generated carrier scheme," *J. Lightw. Technol.* **26**(10), 1249–1255 (2008).
4. S. C. Huang and H. Lin, "Modified phase-generated carrier demodulation compensated for the propagation delay of the fiber," *Appl. Opt.* **46**(31), 7594–7603 (2007).
5. J. He, L. Wang, F. Li, et.al. "An ameliorated phase generated carrier demodulation algorithm with low harmonic distortion and high stability," *J. Lightw. Technol.* **28**(22), 3258–3265 (2010).
6. A. D. Kersey, A. Dandridge, A. B. Tveten. "Time-division multiplexing of interferometric fiber sensors using passive phase-generated carrier interrogation," *Opt. Lett.* **12**(10), 775–777 (1987).
7. A. Dandridge, A. B. Tveten, T. G. Giallorenzi, et.al. "Homodyne demodulation scheme for fiber optic sensors using phase generated carrier," *IEEE J. Quantum. Electron.* **QE-8**(10), 1647–1653 (1982).
8. Y. W. Tong, H. L. Zeng, L. Y. L, and Y. Zhou. "Improved phase generated carrier demodulation algorithm for eliminating light intensity disturbance and phase modulation amplitude variation," *Appl. Opt.* **51**(29), 6962–6967 (2012).
9. Q. P. Shi, Q. Tian. "Performance improvement of phase generated carrier method is eliminating the laser intensity of seismometer," *Optical Engineering.* **49**(2):024402 (2010).
10. G. Q. Wang, T. W. Xu, F. Li. "PGC demodulation technique with high stability and low harmonic distortion," *IEEE Photonic T. L.* **24**(23), 2093–2096 (2012).
11. S. Kobayashi, Y. Yamamoto, T. Kimura. "Modulation frequency characteristics of directly modulated optical frequency modulated AlGaAssemiconductor lasers," *Electron.Lett.* **17**(10), 350–351 (1981).
12. K. Kirkendall, A. Dandridge. "Overview of high performance fiber-optic sensing," *J. Phys. D. Appl. Phys.* **37** (04), 197–216 (2004).